

## Ionization Produced by Atomic Collisions at kev Energies\*

A. RUSSEK AND M. TOM THOMAS  
*The University of Connecticut, Storrs, Connecticut*  
 (Received January 30, 1957)

A phenomenological theory is developed which accounts for the ionization produced by single collisions between heavy atoms or ions at kiloelectron volt energies. The collision ionization is regarded as a two-step process. First, as the two electron distributions sweep through each other, a certain amount of energy is transferred by a friction-like mechanism from the kinetic energy of translation of the atoms to their internal degrees of freedom. Second, this transferred energy, which is analogous to heat energy, is statistically distributed among the electrons. The probability that any given number of electrons acquire more than the ionization energy is then computed by a straightforward statistical

analysis. The probabilities that the collision products are in the various states of ionization are thereby calculated as functions of the collision parameters. This ionization mechanism is analogous to the evaporation of molecules from a heated liquid.

The theory is compared with experiment for the case in which singly charged argon ions are scattered by neutral argon atoms at energies of 25, 50, and 100 kev. At each bombarding energy the probabilities of finding the detected atom in any of the charge states, from zero to seven times ionized, as functions of the angle of scattering are predicted with reasonable accuracy with only two adjustable parameters.

### 1. INTRODUCTION

WHEN two atoms collide at sufficiently high energies, a scattering occurs which can be adequately accounted for in terms of an elastic collision between two shielded point charges.<sup>1</sup> In addition, the scattered systems are found to be in various states of ionization. Recently, considerable experimental data has been accumulated on the scattering of heavy ions by heavy neutral atoms, giving the probabilities of the various states of ionization as functions of the energy and the scattering angle.<sup>2-4</sup>

Inasmuch as a rigorous quantum-mechanical approach to the problem appears to be of prohibitive difficulty, it seems to be a worthwhile endeavor to formulate a phenomenological model of the collision-ionization process at these energies, which correlates the existing experimental data. It is hoped that this will supply an intuitive understanding of the process which may not only provide a framework for conceiving new experiments, but also indicate the approximations most appropriate in an eventual rigorous quantum mechanical approach to the problem.

Basically, in the model suggested by the data, the collision-ionization is regarded as a two-step process. First, as the two charge distributions sweep through each other, a relatively small amount of the kinetic energy of translation of the atoms is transferred to their internal degrees of freedom by a friction-like mechanism. Second, upon separation the "heated" atoms get rid of this excess energy partly by photon emission and partly by electron evaporation. It is to be expected that there will be a statistical distribution in the number of electrons evaporated when a given

amount of energy is transferred to the internal motion of the colliding atoms.

The detailed assumptions which define the proposed model are presented in Secs. 2 and 3. Section 2 deals with the statistical distribution among the orbital electrons of the energy transferred to the internal degrees of freedom. In Sec. 3, the energy transferred to the internal motion is obtained as a function of the collision parameters. In Sec. 4, the theory is compared with experiment in the case of scattering of singly ionized argon atoms incident upon neutral argon atoms at energies of 25, 50, and 100 kev. Agreement with the data is found to be good. In the concluding section, the assumptions made in Secs. 2 and 3 are examined by analyzing the effects on the over-all agreement when they are altered.

### 2. DISTRIBUTION OF THE ENERGY TRANSFERRED

The purpose of this section is to determine how the energy transferred to the internal degrees of freedom is distributed among the electrons. For the sake of explicitness, the present work is restricted to the case in which both atomic particles, target and projectile, have outer shells of eight electrons and in which the translational energy of the projectile is between about 2 kev and 1 Mev. These requirements are fulfilled by the argon-argon collisions for which the theory will be compared with the experimental data.

#### A. Assumptions

Four assumptions are made. They will be discussed below and re-examined in the light of the experimental data in Sec. 5.

- (1) The energy transferred is distributed among the eight outer electrons only.
- (2) The energy transferred is statistically distributed among these electrons. To make the problem tractable, the energy scale is divided into cells of equal width  $\epsilon$ .
- (3) The ratios of the statistical weights of the cells in the bound energy region to those of the cells in the

\* This work was sponsored by the Office of Ordnance Research, U. S. Army, through the Ordnance Materials Research Office at Watertown and the Springfield Ordnance District.

<sup>1</sup> Everhart, Stone, and Carbone, *Phys. Rev.* **99**, 1287 (1955).

<sup>2</sup> Fuls, Jones, Ziembra, and Everhart, *Phys. Rev.* **107**, 704 (1957).

<sup>3</sup> Carbone, Fuls, and Everhart, *Phys. Rev.* **102**, 1524 (1956).

<sup>4</sup> D. M. Kaminker and N. V. Fedorenko, *Zhur. Tekh. Fiz.* **25**, 2239 (1955).

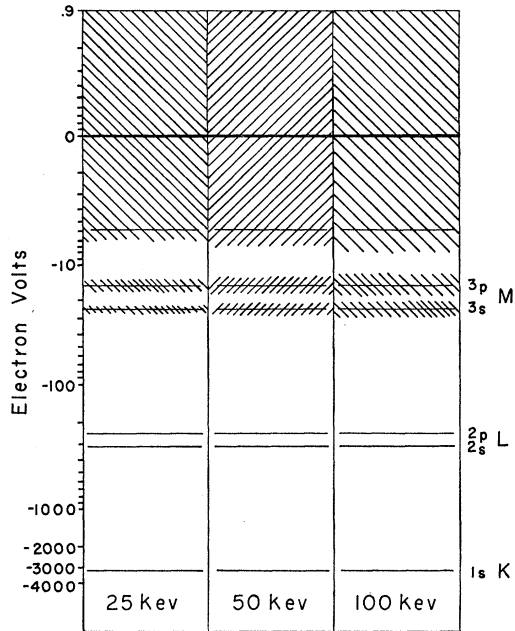


FIG. 1. Broadened energy-level diagrams for neutral argon. The shaded area shows the allowed energy ranges for an individual electron. The vertical axis has  $-(1+E)$  plotted on a logarithmic scale in order to show the entire energy range of interest, including all bound states. For collision times corresponding to each of the three bombarding ion energies, all energy levels were broadened to cover a range  $2\Delta E$ , where  $\Delta E$  is the Heisenberg uncertainty in the energy. The bound excited levels were obtained from that part of the optical spectrum in which one  $3s$  electron is elevated to the respective vacant levels. The lines, wherever drawn, show the original unbroadened levels.

continuum are approximately unity. In other words, all cells are taken to have the same statistical weight.

(4) A uniform ionization energy is assumed. Any of the eight outer electrons that acquire more than this energy will escape regardless of how many others also escape.

The ultimate justification for these assumptions is that they are necessary in order to achieve agreement with the data. Therefore, in Sec. 5, these assumptions are varied and it will there be seen that any significant change either destroys or appreciably reduces the agreement. Nevertheless, the assumptions are intuitively reasonable *a priori*, as the following plausibility argument will show.

The collision process takes place during a finite time  $T = D/v_I$ , where  $D$  is a distance of the order of magnitude of the diameter of an atom and  $v_I$  is the translational velocity of the projectile. Because of the Heisenberg uncertainty principle, each sharp energy level in the discrete part of the spectrum is broadened to an interval of half-width

$$\Delta E \simeq \hbar/T = \hbar v_I/D. \quad (1)$$

For argon-argon collisions at bombarding energies of 25, 50, and 100 keV, for example,  $\Delta E$  is found to be

1.7, 2.4, and 3.4 eV, respectively. The effect of this broadening on the energy spectrum of an isolated argon atom is shown in Fig. 1. Between the first excited state and the ionization energy, the width of the levels is larger than the separation between them so that this portion of the energy spectrum which contains the bound excited states is smeared into a continuum. To be sure, the broadening produced by the uncertainty principle has been applied to the level structure of an isolated atom. The structure will be different for a pair of atoms in close proximity (during the collision), but it is reasonable to assume that the orders of magnitude of the spacings are the same as for the isolated atoms. Thus, it does not appear unreasonable to assume a statistical distribution of the energy transferred with equal statistical weights (assumptions 2 and 3). The lower limit of projectile energy for which these assumptions are expected to be valid is  $\sim 2$  keV at which energy the individual energy levels begin to resolve.

The broadening of the  $K$  and  $L$  energy levels is negligible by comparison with their separations and does not even show up on the logarithmic scale of Fig. 1. Therefore, it would appear that these electrons can adjust adiabatically to the changing potential during the collision. Moreover, if any of these electrons were given any energy at all, they would have to be given an inordinately large amount of energy (enough to raise them to a vacant level). This seems to be a valid argument for restricting the distribution of the energy transferred to the eight outer electrons (assumption 1). The validity of this assumption fixes the upper limit of collision energies at which the model can be expected to hold. It should be noted, however, that the  $K$  and  $L$  electrons can take part in electron-electron collisions to the extent that they can give or receive an energy of the order of magnitude of  $\Delta E$  without leaving their original states. Thus, these electrons can account for a small part of the energy transferred. This point will be discussed further in Sec. 5.

There is no *a priori* justification for assumption 4. If electron evaporation took place long after the atoms separated (i.e., when each was isolated), it would take a minimum of  $\sim 15$  eV to get one electron out,  $\sim 45$  eV to get two electrons out, etc.; that is, the greater the number of electrons which are evaporated, the more energy is required per electron. Such a "staggered ionization energy" is considered in Sec. 5, and it yields results in noticeably poorer agreement with the data. Thus, it appears that evaporation takes place as the two atoms are separating. (It should be pointed out that this is implicitly required by assumptions 2 and 3, for if the evaporation took place long after separation, the uncertainty principle broadening would no longer be valid.) Inasmuch as electron escape appears to take place when the atoms are not isolated, it is plausible that a uniform ionization energy is a better approximation than a staggered ionization energy.

## B. Ionization Probabilities

As noted in assumption 2, the energy scale is divided into cells of equal size  $\epsilon$  and, according to assumption 3, of equal statistical weight. The ionization energy may be taken as a convenient multiple of  $\epsilon$ . Too small a multiple, however, would result in too coarse statistics, whereas a large multiple, although desirable for accuracy, would result in calculations of exorbitant length. As a compromise,  $4\epsilon$  is taken as the ionization energy.

The energy transferred, denoted by  $E_T$ , is considered to be  $m\epsilon$  if  $m\epsilon \leq E_T < (m+1)\epsilon$ , where  $m$  is an integer. It follows from the four assumptions that the probability  $P_n(m)$  that a neutral atom will become  $n$  times ionized if an energy  $E_T = m\epsilon$  is transferred to its internal motion is given by the number of ways in which the energy  $m\epsilon$  can be divided among the eight outer electrons so that  $n$  and only  $n$  electrons have  $4\epsilon$  or more, divided by the total number of ways that the energy  $m\epsilon$  can be divided among eight electrons.

To facilitate the counting, the following quantities will be introduced.

(a)  $K_n(m)$  is the total number of ways in which the energy,  $E_T = m\epsilon$ , can be divided among  $n$  electrons. This is just the number of ways of writing  $m$  as the sum of  $n$  integers (where  $1+2+3$  and  $1+3+2$  are counted as two different ways of writing 6 as the sum of 3 integers).<sup>5</sup>

(b)  $Q_n(m)$  is the number of ways in which the energy  $m\epsilon$  can be divided among  $n$  electrons such that *none have more energy than  $3\epsilon$* . It is the number of ways in which  $m$  can be written as the sum of  $n$  integers, all less than or equal to 3.

With these definitions, the ionization probabilities are found, by elementary algebra, to be

$$P_0(m) = Q_8(m) / K_8(m),$$

$$P_n(m) = \binom{8}{n} \sum_{i=0}^{m-4n} K_n(i) Q_{8-n}(m-4n-i) / K_8(m), \quad (2)$$

where  $\binom{8}{n}$  is the binomial coefficient.

Equations (2) give the probability that when the energy  $m\epsilon$  is distributed among eight electrons,  $n$

<sup>5</sup> The electrons are here treated as distinguishable particles, although they are not, of course, intrinsically distinguishable. However, the eight electrons are initially in eight different angular momentum quantum states, and a distinction can be made in terms of these initial states. Thus, if only one electron escapes, it makes sense to say the electron originally in state such-and-such escaped. In fact, if only one electron is knocked out and the others are unaffected by the collision, the distinction can clearly be made experimentally by noting which quantum state is vacant after the collision. If this reasoning is debatable, it would be well to point out that the above argument is not essential to the validity of the theory. The energy cells are highly degenerate and the occupation numbers small, in which case Fermi-Dirac, Bose-Einstein, and Boltzmann statistics all reduce to a common limit.

electrons will have sufficient energy to get out. The remaining electrons, which are excited but do not have enough energy to escape, will fall back to their ground states, giving up their energy by photon emission. The Pauli exclusion principle does not affect the results given by (2), since only a few electrons are distributed over a large number of cells. Moreover, each cell can accommodate a large number of electrons, equal to the number of individual levels contained within the cell, in the bound region and an infinite number in the continuum.

It remains now to calculate the quantities  $K_n(m)$  and  $Q_n(m)$ , which can be obtained by means of recursion relationships. Suppose that for given  $n$  the  $K_n(m)$  were known for all  $m$ . That is, for  $n$  electrons, the total number of ways of distributing the energy  $m\epsilon$  has been calculated for all  $m$ . It is then possible to calculate  $K_{n+1}(m)$ . The  $n+1$ st electron can be given any energy from  $0\epsilon$  to  $m\epsilon$ . If this electron is given energy  $r\epsilon$ , the remaining  $n$  electrons must share the energy  $(m-r)\epsilon$  and this can be done in  $K_n(m-r)$  ways.

$$K_{n+1}(m) = \sum_{r=0}^m K_n(m-r). \quad (3)$$

To start this chain, it is necessary to have  $K_2(m)$ , the number of ways that  $m\epsilon$  can be divided between two electrons. The first electron can be given energy  $0, \epsilon, \dots, m\epsilon$  (i.e.,  $m+1$  possible values) and, of course, there is then no further choice, since the second electron must take what is left over. Therefore,

$$K_2(m) = m+1. \quad (4)$$

The recursion scheme given by Eqs. (3) and (4) can be solved explicitly:

$$K_n(m) = \left[ \prod_{i=1}^{n-1} (m+i) \right] / (n-1)!. \quad (5)$$

The recursion relationships for the  $Q_n(m)$  can be similarly obtained. If the  $Q_n(m)$  are all known, then  $Q_{n+1}(m)$ , the number of ways  $n+1$  electrons can share  $m\epsilon$  such that none has more than  $3\epsilon$ , can be obtained by giving the last electron any one of the four permitted values of energy,  $0, \epsilon, 2\epsilon$ , or  $3\epsilon$ . The remaining  $n$  electrons must then share the energy  $m\epsilon, (m-1)\epsilon, (m-2)\epsilon$ , or  $(m-3)\epsilon$  in such a way that none has more than  $3\epsilon$ . Thus

$$Q_{n+1}(m) = \sum_{r=0}^3 Q_n(m-r). \quad (6)$$

As can be seen by direct counting,

$$\begin{aligned} Q_2(m) &= m+1 & \text{for } 0 \leq m \leq 3 \\ &= 7-m & \text{for } 4 \leq m \leq 6 \\ &= 0 & \text{for } 7 \leq m. \end{aligned} \quad (7)$$

No explicit solution analogous to Eq. (5) for this recursion scheme was obtained, and the  $Q_n(m)$  had to

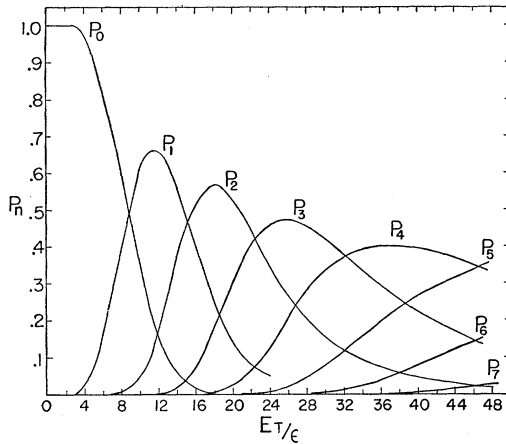


FIG. 2. The ionization probabilities for a neutral atom containing eight electrons in the outer shell are plotted as functions of the energy  $E_T$  transferred to the internal degrees of freedom. The energy is given in units of size  $\epsilon$ ,  $\epsilon$  being one quarter of the average ionization potential of the electrons in the outermost shell.

be tabulated directly from Eqs. (6) and (7). Upon using the values of the  $K_n(m)$  and  $Q_n(m)$  obtained in this manner in Eqs. (2), the ionization probabilities are obtained as functions of  $m = E_T/\epsilon$  and are shown in Fig. 2 for the eight-electron case.

### C. Comparison of Evaporation Theory with Experiment

In order to compare the evaporation theory, just presented, with experiment, account must be taken of the fact that the incoming particle, which is already singly ionized, comes into intimate contact with the electronic shells of a neutral atom. There is an even chance that, upon separation, this single electron deficiency will be associated with either atom. Hence, the probability that the projectile will be singly charged, even before electron evaporation is taken into consideration, is one-half. This modifies the ionization probabilities as calculated in the previous section and presented in Fig. 2.

The modified ionization probability is denoted by  $\tilde{P}_n$ . This is just the probability  $\frac{1}{2}P_n(m)$  that upon separation the observed atom was neutral and evaporated  $n$  electrons plus the probability  $\frac{1}{2}P_{n-1}(m)$  that it was already singly ionized and lost only  $n-1$  electrons.

$$\tilde{P}_n(m) = \frac{1}{2}P_n(m) + \frac{1}{2}P_{n-1}(m). \quad (8)$$

These probabilities are shown in Fig. 3, plotted against the energy transferred  $E_T$  in units of size  $\epsilon$ , this unit being one quarter of the average ionization potential.

In order to compare the theory with the experimental data, the ionization probabilities must be plotted not as functions of  $E_T$ , but as functions of the energy of the incident projectile  $E_I$  and the angle of scattering  $\theta$ . Section 3 which follows is devoted to this aspect of the problem. However, it is evident that  $E_T$  is a monotonic

increasing function of  $\theta$ , for the large deflections  $\theta$  correspond to violent collisions for which  $E_T$  is large, and vice versa. Replotting the ionization probabilities as functions of  $\theta$  instead of  $E_T$  has only the effect of horizontally distorting the curves of Fig. 3 with no change in the vertical direction. If Fig. 3 were reproduced on a sheet of rubber which was capable of being stretched arbitrarily in the horizontal direction but was rigid in the vertical direction, it should be possible for some inhomogeneous horizontal stretching, to make them congruent, at each incident ion energy to a similar figure in which the experimental ionization probabilities are plotted as functions of  $\theta$ . What is being said, in a somewhat pictorial way, is that the evaporation theory just presented predicts, unambiguously and without any parameter adjustments whatever, not only the heights of all the ionization probability curves as well as the height of the intersection of each pair of curves, but also the horizontal order in which they occur.

The evaporation aspect of the model is quite successful as can be seen in Table I. This gives the heights and order of occurrence as  $E_T$  increases. For comparison, the corresponding values, taken from the experimental results of reference 2, for collisions of  $A^+$  on  $A$  at 25, 50, and 100 kev, are listed in order of increasing deflection  $\theta$ . Agreement between theory and experiment is seen to be quite good. Indeed, the agreement between the experimental curves, themselves, at the three different energies (insofar as heights of peaks and intersections and order of occurrence is concerned) constitutes a verification of the evaporation theory. Despite the difference in appearance of the sets of experimental curves shown in Fig. 4 (reproduced from reference 2), they are all essentially horizontal distortions of a single set of curves, as Table I indicates. With a single exception, the experimental peak and intersection heights at the three different energies agree with each other to within 0.05, and the theoretical values for these points agree with the average of the experimental values to within 0.04, the mean dis-

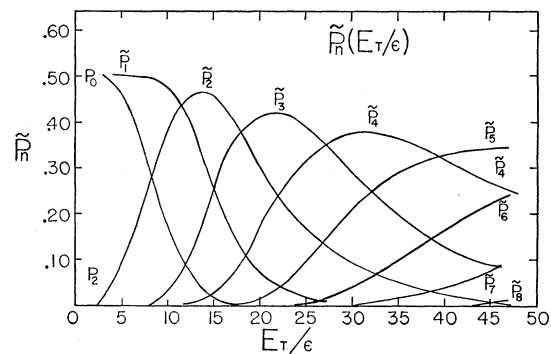


FIG. 3. The modified ionization probabilities,  $\tilde{P}_n$ , defined by Eq. (8) in the text. These are needed for the scattering of singly ionized atoms by neutral atoms of the same type.

crepancy being 0.02. These discrepancies are quite small, by comparison with 0.5, the approximate height these curves achieve.

3. ENERGY TRANSFERRED

The purpose of this section is to obtain a measure of the energy  $E_T$  transferred to the electrons during the collision. The energy transfer process is assumed to consist of a number of two body electron-electron collisions which jar the colliding electrons out of their initial orbits into those of higher energy. This assumption (number 5) takes the mathematical form

$$E_T(E_I, r_0) = e_T(E_I) \nu(E_I, r_0), \quad (9)$$

where  $e_T$  is the average energy acquired by each electron in an electron-electron collision and  $\nu$  gives the number of such collisions that take place during the over-all atomic collision. The collision parameters are the energy  $E_I$  of the incident projectile in the laboratory reference frame, and the distance  $r_0$  of closest approach of the two nuclei.

Two assumptions are implicitly made when  $E_T$  is expressed in the form of Eq. (9).

(5a) The electrons can adjust adiabatically to the nuclear motions, so that the energy transferred is primarily due to electron-electron collisions. This is equivalent to assuming that the orbital velocities are large compared to the relative velocity of the atoms.

(5b) An electron-electron collision transfers a significant amount of energy to the internal motion only if the impact parameter of this collision is less than some fixed length  $L$  which is small compared to the

TABLE I. Heights of intersections and peaks of the theoretical ionization probability curves compared with the experimental values.

Intersection or peak <sup>a</sup>	Experimental values <sup>b</sup>			Theoretical values <sup>c</sup>
	25 kev	50 kev	100 kev	
$\bar{P}_2 \times \bar{P}_1$	0.42	...	...	0.42
$\bar{P}_3 \times \bar{P}_0$	0.09	0.07	...	0.09
$\bar{P}_2$	0.42	0.51	...	0.46
$\bar{P}_3 \times \bar{P}_1$	0.24	0.22	...	0.25
$\bar{P}_4 \times \bar{P}_0$	0.07	0.05	...	0.02
$\bar{P}_3 \times \bar{P}_2$	0.34	0.33	0.36	0.39
$\bar{P}_4 \times \bar{P}_1$	0.15	0.13	0.13	0.11
$\bar{P}_3$	0.41	0.38	0.36	0.42
$\bar{P}_4 \times \bar{P}_2$	0.23	0.24	0.24	0.25
$\bar{P}_5 \times \bar{P}_0$	...	0.03	...	0.00
$\bar{P}_4 \times \bar{P}_3$	...	0.33	0.32	0.35
$\bar{P}_5 \times \bar{P}_2$	...	0.13	0.14	0.13
$\bar{P}_6 \times \bar{P}_1$	...	0.02	0.02	0.01
$\bar{P}_4$	...	0.38	0.37	0.37
$\bar{P}_5 \times \bar{P}_3$	...	...	0.24	0.24
$\bar{P}_6 \times \bar{P}_2$	...	...	0.06	0.07
$\bar{P}_5 \times \bar{P}_4$	...	...	0.32	0.32
$\bar{P}_6 \times \bar{P}_3$	...	...	0.14	0.14
$\bar{P}_7 \times \bar{P}_2$	...	...	0.04	0.03
$\bar{P}_5$	...	...	0.35	0.35
$\bar{P}_6 \times \bar{P}_4$	...	...	0.24	0.24

<sup>a</sup>  $\bar{P}_2 \times \bar{P}_1$  refers to the height of the intersections of the curves  $\bar{P}_2$  and  $\bar{P}_1$ , etc.  $\bar{P}_2$  refers to the height of the peak of the curve  $\bar{P}_2$ , etc.  
<sup>b</sup> Taken from Fig. 4.  
<sup>c</sup> Taken from Fig. 3.

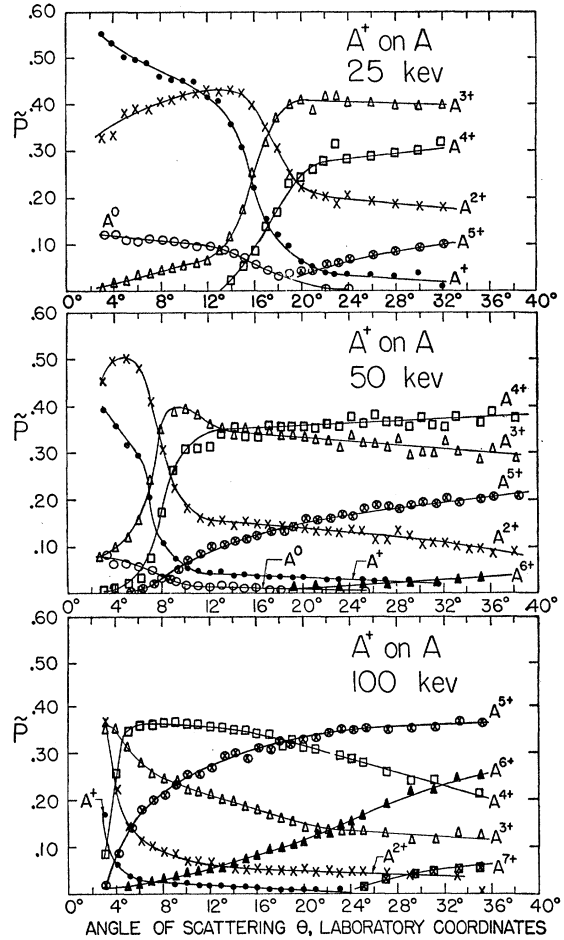


FIG. 4. The experimental ionization probabilities for  $A^+$  on  $A$  at energies of 25, 50, and 100 kev taken from reference 2, are here shown plotted as functions of  $\theta$  the angle of scattering in laboratory coordinates.

size of the atom. The forces between charges at larger separations combine to form an average force on each charge which contributes to the deflection of each atom as a whole by the collision. As a consequence of this assumption, forces due to all other charges can be neglected during each electron-electron collision, thereby justifying the expression of  $E_T$  in terms of two-body collisions.

As a rough approximation, the energy transferred per electron-electron collision will be taken to be the average energy possessed by each electron in one atom with respect to a frame fixed in the second atom,

$$e_T(E_I) = \langle \frac{1}{2} m (\mathbf{v}_0 + \mathbf{v}_I)^2 \rangle = e_0 + (m/M) E_I. \quad (10)$$

This is the average energy which each electron has as it smashes through the other atom. Here  $\mathbf{v}_0$  and  $e_0$  denote average orbital velocity and energy respectively,  $m$  and  $M$  represent the electron and atom masses respectively, and  $\mathbf{v}_I$  and  $E_I$  the velocity and energy of the incident projectile. It should be stressed that Eq. (10) is not an assumption, but rather, an approximation.

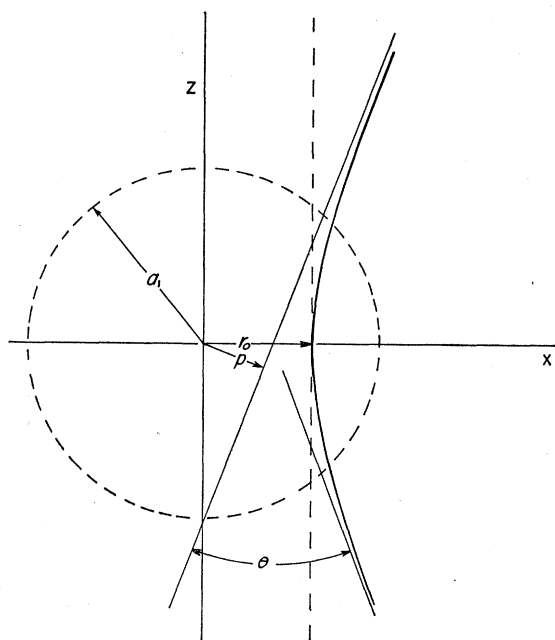


FIG. 5. A typical scattering event. The actual path of the incident atom is shown as a solid line, while the dotted straight line parallel to the  $z$  axis at distance  $r_0$  is the approximate path used in the theory. In the region in which the charge density is appreciable (within the circle), the two paths do not differ greatly.

A typical scattering event is shown in Fig. 5, where the actual path of the incident atom is shown as a solid line. The dotted straight line parallel to the  $z$  axis at distance  $r_0$  closely approximates this path in the region in which the charge densities appreciably overlap. This straight line path, which may be taken parallel to the  $z$  axis for convenience, can therefore be used to simplify the calculation of the number of electron-electron collisions  $\nu$ . The latter quantity is equal to the number of electrons of one atom which sweep past any electron of the other atom with a distance of closest approach less than or equal to  $L$ . Since all of the electrons in a cylinder parallel to the  $z$  axis will sweep past any point with the same minimum distance, as can be seen in Fig. 6, it is convenient to introduce the density function  $\sigma(x, y)$  for either atom, where  $\sigma(x, y) dx dy$  gives the number of electrons in one of the cylinders of cross-sectional area  $dx dy$  shown on the figure. This number of electrons is

$$\sigma(R) = \int_{-\infty}^{+\infty} \rho(r) dz, \quad (11)$$

where  $R = (x^2 + y^2)^{\frac{1}{2}}$  and  $r = (x^2 + y^2 + z^2)^{\frac{1}{2}}$ . Here,  $\rho$  is the number of electrons per unit volume. The density  $\sigma$  is, then, just the area density that would result if the atom were squashed flat in a plane perpendicular to the direction of motion, as shown in Fig. 6. For this reason,  $\sigma$  will be referred to as the "squashed density." It should be pointed out that  $\rho$  and  $\sigma$  should properly

refer, not to over-all densities, but only to the densities of those electrons allowed to participate in collisions; i.e.,  $M$ -shell electrons.

The number of collisions  $\nu$  is essentially just the number of electron pairs, one from each "squashed" atom, which lie within a distance  $L$  of each other in the plane into which the two atoms have been squashed. In fact,  $\nu$  is given by this quantity except for a multiplicative function  $g(E_I)$  to be discussed presently. Thus

$$\nu = g(E_I) \int \sigma_1(x_1, y_1) \sigma_2(x_2, y_2) f(R_{12}) dx_1 dy_1 dx_2 dy_2, \quad (12)$$

where

$$R_{12} = [(x_1 - x_2)^2 + (y_1 - y_2)^2]^{\frac{1}{2}}, \quad (13)$$

$$f(R_{12}) = 1 \quad \text{if } R_{12} \leq L \\ = 0 \quad \text{if } R_{12} > L, \quad (14)$$

and  $\sigma_1$  and  $\sigma_2$  are the squashed densities of the two atoms. If these density functions do not vary rapidly over distances comparable with  $L$ , the theorem of the mean may be employed to simplify the result. Thus,  $f(R_{12})$  will be approximated by a multiple of the Dirac  $\delta$  function,  $\pi L^2 \delta(R_{12})$ . Integrating over  $x_2, y_2$  and replacing  $x_1, y_1$ , by  $x, y$ ,

$$\nu = \pi L^2 g(E_I) M(r_0), \quad (15)$$

where

$$M(r_0) = \int \sigma_1(x, y) \sigma_2(x, y) dx dy. \quad (16)$$

In the above description, it was implicitly assumed that the electrons did not move in their respective orbits as the two atoms sweep through each other. The orbital motion of the electrons will increase the number of electron collisions. This can best be seen by imagining a very slow atomic collision. During the time of sweep-through, each electron will make several revolutions, so that the same pair of electrons may bump into each other several times during the collision. The factor

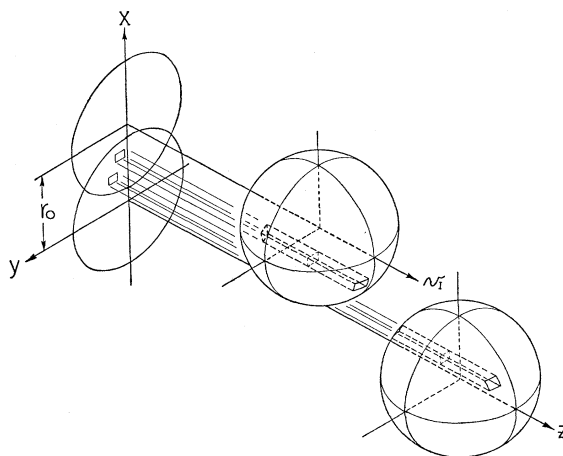


FIG. 6. A three-dimensional view of the scattering event shown in Fig. 5.

$g(E_I)$  gives the dependence of the number of electron-electron collisions on the incident ion energy. For an infinitely fast collision it should reduce to unity, since the remaining factors in Eq. (15) were derived on the basis of electrons fixed in their respective atoms during the collision. The increase in the number of collisions due to a finite collision time is expected to be proportional to the time of collision. Therefore, it is reasonable to assume that  $g(E_I)$  has the form:

$$g(E_I) = 1 + B'/v_I = 1 + BE_I^{-\frac{1}{2}}, \quad (17)$$

where  $B$  is an undetermined positive parameter.

With Eqs. (10), (15), and (17) substituted into Eq. (9),  $E_T$  then has the form:

$$E_T(E_I, r_0) = A(1 + mE_I/M e_0)(1 + BE_I^{-\frac{1}{2}})M(r_0), \quad (18)$$

where,  $e_0\pi L^2$  has been replaced by the second undetermined parameter  $A$ . This involves no loss of information, inasmuch as  $L$  is also undetermined.

Equation (18) gives the energy transferred as a function of  $E_I$  and  $r_0$ , while the experimental data is given in terms of  $E_I$  and  $\theta$ . However  $r_0$  is a known function of  $E_I$  and  $\theta$ , (see reference 1) so that Eq. (18) can be re-expressed in terms of the proper variables with no further assumptions required. This is done in the following section.

It may be noted, at this point, that the parameter  $A$  and the unknown ionization energy of the previous section actually constitute but a single adjustable parameter, inasmuch as only the ratio of the two enters into the theory. Therefore  $A/\epsilon$  and  $B$  are the only two adjustable parameters of the theory.

#### 4. COMPARISON WITH EXPERIMENT

The complete theory described above will now be compared with experiment for the case in which singly ionized argon atoms are scattered off neutral argon atoms at bombarding energies of 25, 50, and 100 kev.

Figure 7(a) shows the radial distribution of electrons  $4\pi r^2\rho$ , where  $\rho$  is the number density, which follows from a Hartree self-consistent calculation for neutral argon. The part due to  $M$ -shell electrons only is required by the theory of Secs. 2 and 3 and is shown as a solid curve. The broken curves show the distributions due to  $(L+M)$ -shell and  $(K+L+M)$ -shell electrons, for comparison. The abscissa in this figure is  $r/a_1$ , where  $a_1$  is  $a_0/Z^{\frac{1}{2}}$ ,  $a_0$  being the radius of the first Bohr orbit in hydrogen. A numerical integration of  $\rho$ , as indicated in Eq. (11), results in the squashed density  $\sigma$ . The squashed densities which follow from the three distributions described above are shown in Fig. 7(b). Again, the one required by the theory is shown as a solid curve.

With this squashed density, the function  $M(r_0)$  is computed by means of Eq. (16). This was done for nine values of the parameter  $r_0$  in the range  $0 \leq r_0 \leq 2a_1$ . The solid curve of Fig. 8 shows the function  $M$ , for  $M$ -shell electrons only, plotted in terms of the dimensionless variable  $r_0/a_1$ . Next,  $M(r_0)$  is expressed as a function of angle of scattering and energy by determining the dependence of  $r_0$  on  $\theta$  for each of the bombarding ion energies. This dependence is shown in Fig. 9, the curves being interpolated from the results obtained by Everhart, Stone, and Carbone<sup>1</sup> and tabulated in Table I of that paper, after converting to the laboratory coordinates for the angle of scattering. It should be noted that the length  $a$  defined in their paper is not the same as  $a_1$  defined here. In fact,  $a_1 = a\sqrt{2}$  in this case.

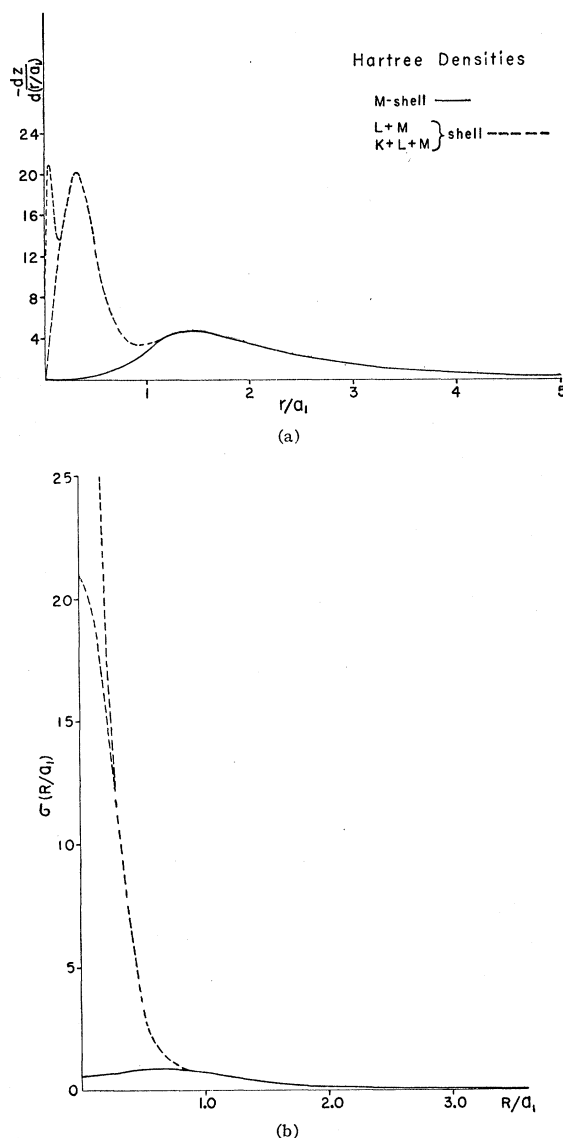


FIG. 7. (a) shows the radial charge distribution  $-dZ/dr = 4\pi r^2\rho$  that follows from a Hartree self-consistent calculation. The  $M$ -shell distribution is shown by the solid curve, while the broken curves show the distributions that result from  $L+M$  and  $K+L+M$  electrons. The abscissa is given in terms of the dimensionless variable  $r/a_1$ . (b) shows the squashed densities  $\sigma$ , defined by Eq. (11) in the text, that follow from each of the above distributions. Again the  $M$  shell is designated by the solid curve. The abscissa is given in terms of the dimensionless variable  $R/a_1$ .

tionless variable  $r_0/a_1$ . Next,  $M(r_0)$  is expressed as a function of angle of scattering and energy by determining the dependence of  $r_0$  on  $\theta$  for each of the bombarding ion energies. This dependence is shown in Fig. 9, the curves being interpolated from the results obtained by Everhart, Stone, and Carbone<sup>1</sup> and tabulated in Table I of that paper, after converting to the laboratory coordinates for the angle of scattering. It should be noted that the length  $a$  defined in their paper is not the same as  $a_1$  defined here. In fact,  $a_1 = a\sqrt{2}$  in this case.

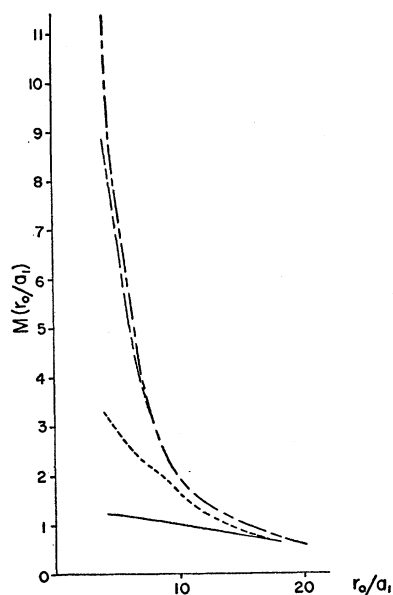


FIG. 8. The function  $M$ , defined by Eq. (16) in the text, is plotted in terms of the dimensionless variable  $r_0/a_1$ . Again, the solid curve follows from the  $M$ -shell distribution, while the two broken curves follow from the  $(L+M)$ -shell and  $(K+L+M)$ -shell distributions. The dashed curve has been empirically determined as the one which most nearly gives the empirically determined  $E_T$  of Fig. 10.

The energy transferred  $E_T$  is obtained using Figs. 8 and 9 with Eq. (18), when the two undetermined parameters  $A$  and  $B$  are specified. The determination of  $A$  and  $B$  is accomplished by finding empirically the function  $E_T(\theta, E_I)$  which, when used with Fig. 3, gives best agreement with the experimental data. The empirical curves are shown as the dotted lines of Fig. 10. The solid lines of this figure are the best approximation to these curves permitted by the theory described above, and are obtained by setting  $A = 24.8\epsilon a_1^2$ ,  $B = 0$ . (For argon  $e_0 \sim 15$  ev.) The adjustment of  $A$  automatically expresses  $E_T$  in  $\epsilon$  units, thereby relating the undetermined ionization energy of Sec. 2 (which

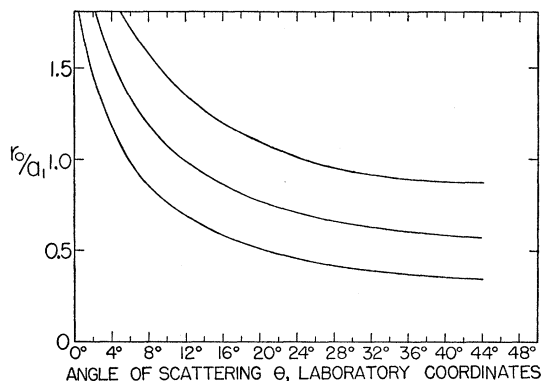


FIG. 9. The distance of closest approach,  $r_0$ , is here plotted in units of size  $a_1$  as a function of the angle of scattering in laboratory coordinates,  $\theta$ , for each bombarding ion energy.

was taken to be  $4\epsilon$ ) to the electron-electron impact parameter  $L$  discussed in assumption 5b. The parameter  $B$  fixes the dependence of the number of electron-electron collisions on the time of sweep through. Although the best value for  $B$  is here found to be zero, it is nonvanishing, if an improved  $M(r_0)$ , discussed below, is used.

With the function  $E_T(\theta, E_I)$  obtained by the method described above, the value of  $\theta$  corresponding to each value of  $E_T/\epsilon$  was read off, and the abscissas of the ionization probability curves shown in Fig. 3 changed to  $\theta$ . The ionization probabilities replotted with the abscissas linear in  $\theta$ , are shown in Fig. 11 along with the experimental data taken from Fuls, Jones, Ziembra, and Everhart<sup>2</sup> and Jones, Ziembra, Moses, and Everhart.<sup>6</sup>

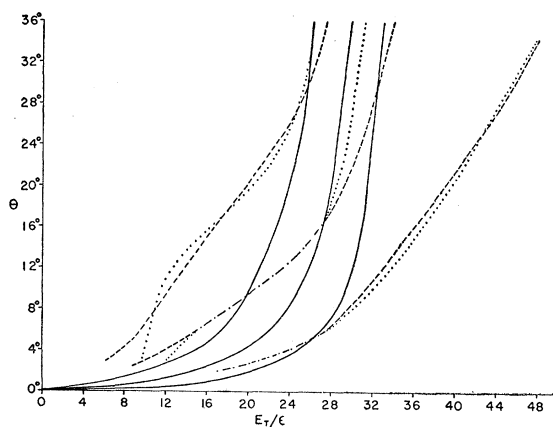


FIG. 10. The energy transferred to the internal degrees of freedom  $E_T$  is shown as a function of  $\theta$  for each bombarding ion energy. The solid curves follow from the theory of Sec. 3, using  $M$ -shell electrons only. The dotted curves are empirically determined curves to yield the best agreement of the evaporation theory of Sec. 2 with the experimental data. The dashed curves show the closest approximation to the empirically determined curves obtainable from the theory of Sec. 3, but using a charge distribution and consequent  $M(r_0/a_1)$  intermediate between that which follows from  $M$ -shell electrons only and  $(L+M)$ -shell electrons.

The good agreement shown in Fig. 11 has been achieved with an *a priori* model of the collision process containing only two adjustable parameters. The data that is correlated consists of 24 curves (eight ionization probabilities plotted as functions of  $\theta$  for each incident ion energy). Not only has the over-all shape and order of magnitude of each curve been reproduced, but also the heights of the peaks are in good agreement with the data. Although it cannot be seen in Fig. 11, the relative position of each curve among its neighbors has been successfully predicted. (The position at which, say, the curve  $P_2$  intersects the curve  $P_3$  defines an intrinsic point on each curve, regardless of whether the axes are given as functions of  $\theta$  or  $E_T$ , and it can be seen from

<sup>6</sup> The data taken at scattering angles below  $4^\circ$  have not yet been published and the authors are indebted for prepublication communication of these results.

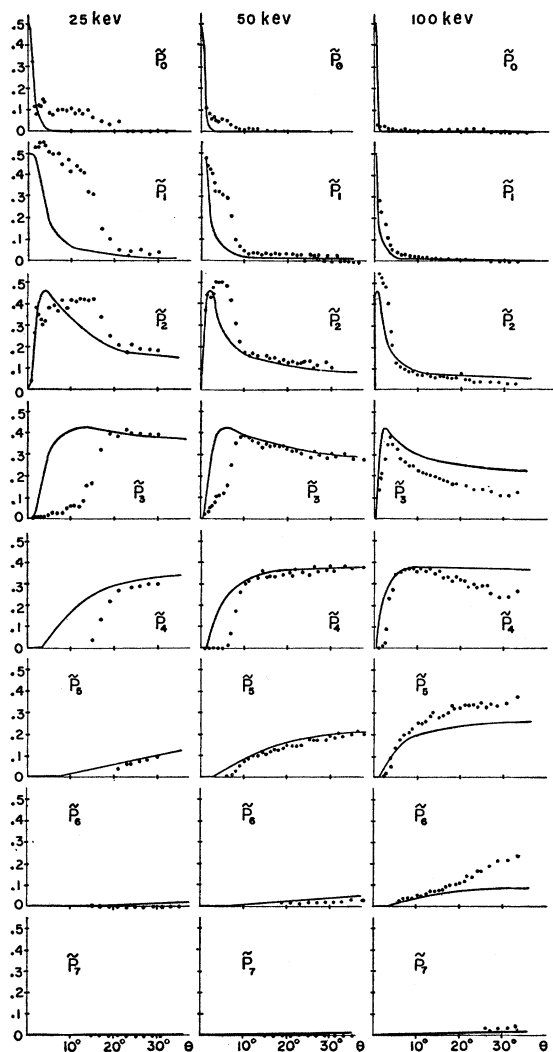


FIG. 11. The ionization probabilities are plotted as functions of  $\theta$  for each bombarding ion energy. These result when functional dependence of  $E_T$  on  $\theta$  is that given by the theory of Sec. 3 (the solid curves of Fig. 10). This illustrates the agreement obtained in comparing the entire theory with experiment.

Table I that the heights of these intersections are successfully predicted.)

The major source of discrepancy lies in the calculation of the energy  $E_T$  transferred to the internal motion by the collision and, in particular, with the assumption that only  $M$ -shell electrons participate in electron-electron collisions. If, instead of using the function  $M(r_0)$  calculated with  $M$ -shell electrons only in Eq. (18), the function shown by the dashed curve of Fig. 8 is substituted, the energy transferred is that given by the dashed curves of Fig. 10, after readjustment of  $A$  and  $B$  to  $13.0\epsilon a_1^2$  and  $7.90 \text{ ev}^{\frac{1}{2}}$  respectively. This corresponds to allowing  $K$  and  $L$  electrons to participate, to a limited extent, in electron-electron collisions, as can be seen in Fig. 8. The consequent agreement

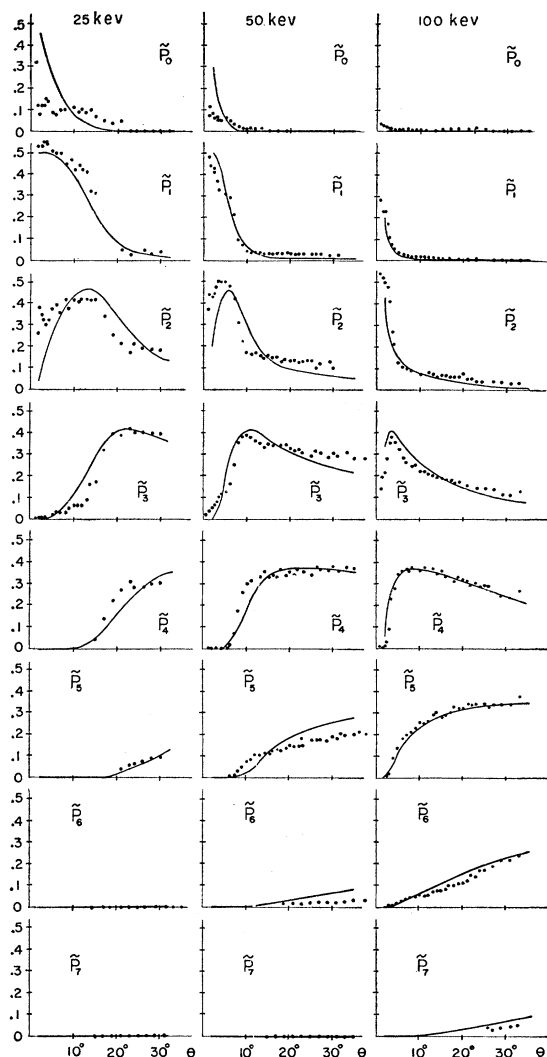


FIG. 12. The ionization probabilities are plotted as functions of  $\theta$  for each bombarding ion energy. These result when the functional dependence of  $E_T$  on  $\theta$  is that given by the dashed curves of Fig. 10. This illustrates the agreement obtainable by the theory, but using a charge distribution and consequent  $M(r_0/a_1)$  intermediate between that which follows from  $M$ -shell electrons only and  $(L+M)$ -shell electrons.

between theory and experiment, which is markedly improved, is shown in Fig. 12.

Before concluding this section, it is appropriate to compare the values of the parameters  $A$  and  $B$  as obtained by empirical adjustment to the orders of magnitude expected on *a priori* grounds. The parameter  $A$  of Sec. 3 is equal to  $\pi L^2 e_0$ , where  $L$  is the impact parameter for electron-electron collisions below which an appreciable fraction of the momentum transfer will be of the random, thermal type, and  $e_0$  is the orbital kinetic energy of  $M$ -shell electrons. By adjustment,  $A$  was found to be of the order of magnitude  $20\epsilon a_1^2$ , where  $\epsilon$  is one quarter of the ionization energy. Taking the ionization energy to be approximately equal to the

first ionization energy of a neutral atom,  $\sim e_0$ , and equating the empirical value to the above expression for  $A$ ,

$$20(e_0/4)a_1^2 = \pi L^2 e_0,$$

from which it is found that  $L = 1.3a_1$ . This is indeed a reasonable size for a length which should be small, but not negligible compared to the size of the atom.

The term  $B/E_I^{3/2}$  of Eq. (17) might naively be expected to be roughly equal to the number of orbital revolutions made by an  $M$ -shell electron during the time of collision. Taking the time of collision to be equal to the time it takes for the nucleus to travel a distance equal to the diameter of the  $M$  shell, the number of revolutions completed during the collision time is found to be 2.1, 1.5, and 1.1 revolutions at 25, 50, and 100 kev, respectively. This would yield a theoretical value for  $B \sim 330 \text{ ev}^{3/2}$  as compared to the value  $7.9 \text{ ev}^{3/2}$  obtained by empirical adjustment. However, it should be noted that at all of the bombarding energies considered, an  $M$ -shell electron makes at least one revolution, so that each of the electrons might be supposed to make at least one collision during the time the atoms are in contact. Inasmuch as just one electron-electron collision transfers nearly all the orbital kinetic energy of the affected electron into the "thermal" energy  $E_T$ , the effectiveness of successive collisions in increasing  $E_T$  is relatively small. Therefore, the effective value for  $B$  should be much smaller than that obtained by merely considering the dependence of the number of electron-electron collisions on the time of collision.

### 5. ANALYSIS OF THE ASSUMPTIONS

In Secs. 2 and 3, a model of the collision-ionization process was proposed via five assumptions. It was seen, in the previous section, that they yield good agreement with the data. However, before concluding that they are supported by the data, it is worthwhile examining the necessity of these assumptions by varying them and noting the effects produced thereby on the over-all agreement with the data.

#### A. Concerning Assumption 1

This assumption stated that primarily the eight  $M$ -shell electrons, took part in the electron-electron collisions. However, it was pointed out that the uncertainty principle broadening of the energy levels would permit the  $K$ - and  $L$ -shell electrons also to participate to a limited extent in these collisions. In order to examine the validity of this assumption, not only was the function  $M(r_0)$  calculated using just the  $M$ -shell electrons, but also similar calculations were performed using  $L$ - and  $M$ -shell electrons as well as  $K$ -,  $L$ -, and  $M$ -shell electrons (i.e., the over-all density). These curves are all shown in Fig. 8. In addition, Fig. 8 contains an empirically determined function  $M(r_0)$  which, when used with Eq. (18), yields the energy transferred  $E_T(\theta, E_I)$ , shown by the dashed curves of

Fig. 10, which most closely approximates the empirically obtained function  $E_T$ , shown by the dotted curves. It is seen in Fig. 8 that the effect of including collisions of the inner electrons is to give the function  $M(r_0)$  a steeper slope for small values of  $r_0$ . It is also seen that the empirically determined curve lies between the one obtained using  $M$ -shell electrons only and those obtained when inner electrons are included, but that it lies closer to the former. This would appear to lend some support to the assumption and the reasoning behind it.

#### B. Concerning Assumption 3

Assumption 3 holds that the statistical weights of the cells in the bound electron energy range ( $< 4\epsilon$ ) are approximately equal to the statistical weights of cells in the free electron energy range ( $\geq 4\epsilon$ ). To test this assumption the following variation was considered:

The four cells in the bound energy range were taken to have the same weight  $w$  relative to the weight of a continuum cell. Thus,  $w$  represents some sort of average statistical weight of these four cells. It then follows that the ionization probabilities are given by

$$\bar{P}_n'(m) = \frac{1}{2}P_n'(m) + \frac{1}{2}P_{n-1}'(m), \quad (19)$$

where  $P_n'$  is given by the following modification of the  $P_n$  defined by Eq. (2):

$$P_n'(m) = w^{8-n}P_n(m) / \sum_{r=0}^8 w^{8-r}P_r(m). \quad (20)$$

TABLE II. Comparison of theoretical heights of intersections and peaks for various statistical weights with the average experimental value.

Intersection or peak <sup>a</sup>	Av. exp. value <sup>b</sup>	Theoretical value				
		$w = 1.25$	1.00	0.715	0.500	0.100
$\bar{P}_2 \times \bar{P}_1$	0.42	0.42	0.42	0.42	0.42	0.45
$\bar{P}_3 \times \bar{P}_0$	0.08	0.08	0.09	0.08	0.08	0.05
$\bar{P}_2$	0.47	0.46	0.46	0.47	0.46	0.50
$\bar{P}_3 \times \bar{P}_1$	0.23	0.25	0.25	0.25	0.25	0.24
$\bar{P}_4 \times \bar{P}_0$	0.06	0.02	0.02	0.02	0.02	0.00
$\bar{P}_3 \times \bar{P}_2$	0.34	0.38	0.39	0.39	0.39	0.42
$\bar{P}_4 \times \bar{P}_1$	0.14	0.11	0.11	0.10	0.10	0.07
$\bar{P}_3$	0.37	0.42	0.42	0.43	0.43	0.47
$\bar{P}_4 \times \bar{P}_2$	0.24	0.25	0.25	0.25	0.25	0.25
$\bar{P}_5 \times \bar{P}_1$	0.06	0.04	0.04	0.04	0.03	0.02
$\bar{P}_4 \times \bar{P}_3$	0.33	0.36	0.35	0.36	0.37	0.41
$\bar{P}_5 \times \bar{P}_2$	0.14	0.13	0.13	0.13	0.13	0.09
$\bar{P}_6 \times \bar{P}_1$	0.02	0.01	0.01	0.01	0.01	0.00
$\bar{P}_4$	0.37	0.37	0.37	0.39	0.40	0.45
$\bar{P}_5 \times \bar{P}_3$	0.24	0.25	0.24	0.25	0.25	0.25
$\bar{P}_6 \times \bar{P}_2$	0.06	0.07	0.07	0.06	0.05	0.02
$\bar{P}_5 \times \bar{P}_4$	0.32	0.32	0.32	0.33	0.34	0.38
$\bar{P}_6 \times \bar{P}_3$	0.14	0.15	0.14	0.14	0.14	0.11
$\bar{P}_7 \times \bar{P}_2$	0.04	0.03	0.03	0.03	0.02	0.00
$\bar{P}_5$	0.35	0.35	0.35	0.35	0.36	0.43
$\bar{P}_6 \times \bar{P}_4$	0.24	0.24	0.24	0.24	0.24	0.24
Mean discrepancy		0.015	0.014	0.017	0.020	0.045

<sup>a</sup>  $\bar{P}_2 \times \bar{P}_1$  refers to the height of the intersection of the curves  $\bar{P}_2$  and  $\bar{P}_1$ , etc.  $\bar{P}_2$  refers to the height of the peak of the curve  $\bar{P}_2$ , etc.

<sup>b</sup> The average is taken over the appropriate experimental values listed in Table I.

That is, for each of the  $8-n$  electrons which end up in the first four cells and are therefore not evaporated, a factor  $w$  must multiply the probability. The denominator, which is the same for all values of  $n$ , merely normalizes the probabilities.

A number of statistical weights were tried about the value of unity required by the theory. The results are compared with experiment in Table II which lists the heights of the peaks as well as the heights of the intersections of the computed ionization probability curves for statistical weights of 1.25, 1.00, 0.715, 0.500, 0.100. These are compared with the average values of the corresponding experimental quantities, the average being taken over the values obtained at each bombarding ion energy. Primary interest was focused on statistical weights of the bound cells less than unity, inasmuch as deviations would be expected in this direction. (Some of the energy range between the highest filled level and the ionization energy is not covered by any broadened level.) The mean discrepancy is seen to be least for  $w=1.00$ , although there is hardly enough difference between the weights 1.25, 1.00, and 0.715 to choose between them. The weights 0.500 and 0.100 are, however, eliminated.

### C. Concerning Assumption 4

This assumption states that the amount of energy needed by any electron to escape is independent of the number of electrons that escape. Intuitively, however, this is not the most reasonable assumption. Rather, it might be expected that the energy needed by any electron to escape would increase as the number of escaping electrons increases. For example, in an isolated neutral argon atom, one electron would need  $\sim 15$  ev to escape; two electrons would need a minimum of  $\sim 43$  ev to escape; three would need a minimum of  $\sim 84$  ev to escape, and so forth. An evaporation model which simulates such a "staggered" ionization energy was considered. If only one electron escapes it requires an energy of  $4\epsilon$  or more; if two electrons escape, they each need  $6\epsilon$  or more, etc. Thus a different ionization energy  $E_n^{(\text{ion})}$  is used for each ionization state  $P_n$  of the neutral atom. This is taken to be the average minimum ionization energy per electron needed to ionize  $n$  electrons, so that  $E_1^{(\text{ion})}=15/1$  ev  $=4\epsilon$ ,  $E_2^{(\text{ion})}=43/2$  ev  $=6\epsilon$ , etc. Upon using this criterion to determine in which ionization state a given distribution would result, it was found that a small percentage of the ways of distributing  $E_T$  were not included in any of the ionization probabilities as defined above. These had to be counted individually and were credited toward the various ionization probabilities by a rather complicated supplementary condition. The results are, however, relatively independent of the details of this condition.

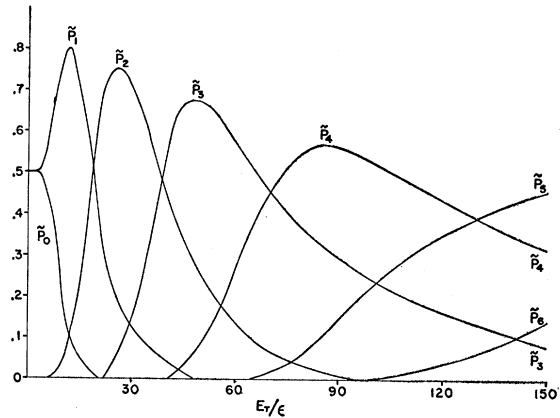


Fig. 13. The ionization probabilities  $\bar{P}_n^{(s)}$  that result when a staggered ionization energy as described in Sec. 5 is used instead of the uniform ionization energy assumed in Sec. 2. These are plotted as function of  $E_T/\epsilon$ .

The final  $\bar{P}_n(m)$  were obtained by averaging for each  $m$  the ionization probability  $P_n(m)$  of a neutral atom with the corresponding ionization probability  $P_{n-1}^*(m)$  for an atom which was initially singly ionized before receiving the energy  $m\epsilon$ :

$$\bar{P}_n(m) = \frac{1}{2}P_n(m) + \frac{1}{2}P_{n-1}^*(m).$$

The  $P_n^*$  were calculated in a manner similar to that described for obtaining  $P_n(m)$ .

The results are presented in Fig. 13 which shows the ionization probabilities as functions of  $E_T/\epsilon$ . Even a cursory glance at this figure is sufficient to observe that this model cannot possibly account for the experimental results. Peak heights are much too large, a large fraction of the intersections of experimental curves do not even occur in Fig. 13, and many more deficiencies are immediately apparent. Nor does any statistical weight from 0.1 to 10 improve the agreement. The fact that the uniform ionization of assumption 4 gives much better agreement with the data than the staggered ionization energy considered above shows that the results are quite sensitive to this assumption.

### 6. ACKNOWLEDGMENTS

The authors would like to thank Dr. Edgar Everhart for many stimulating discussions and for his many critical comments at all stages of the work. Thanks are also due Dr. Robert Carbone for suggestions at the early stages of the work. Inasmuch as the theory was improved and developed as new and more accurate data was accumulated, the patient explanations of the experimental data given by Ellis N. Fuls, Francis P. Ziemba, and Phillips R. Jones were particularly invaluable.